Contribution from the Laboratoire de Chimie Organo-Minerale, Institut de Chimie, Université Louis Pasteur, F-67000 Strasbourg, France, and Istituto FRAE-CNR and Dipartimento di Chimica "G. Ciamician" dell' Università, 40126 Bologna, Italy

Photoinduced Processes in Dyads and Triads Containing a Ruthenium(II)-Bis(terpyridine) Photosensitizer Covalently Linked to Electron Donor and Acceptor Groups

Jean-Paul Collin,*[1a] Stephane Guillerez,[1a] Jean-Pierre Sauvage,*[1a] Francesco Barigelletti,*[1b] Luisa De Cola,[1c] Lucia Flamigni,[1b] and Vincenzo Balzani[1c]

Received March 28, 1991

Five supramolecular systems containing the $Ru(ttp)_2^{2+}$ photosensitizer (P) covalently linked to an electron acceptor (A), MV^{2+}, and/or an electron donor (D), PTZ or DPAA, have been synthesized; ttp is 4'-*p*-tolyl-2,2':6',2''-terpyridine, MV^{2+} is methyl viologen, PTZ is phenotiazine, and DPAA is di-*p*-anisylamine. In the D-P-A triads the electron donor and acceptor groups are linked in opposite positions with respect to the photosensitizer. The spectroscopic properties (room-temperature absorption spectra, emission spectra and lifetimes in the 90-200 K temperature range, and transient absorption spectra and lifetimes at 150 K) and the (room-temperature) electrochemical behavior of the supramolecular systems and of their components have been investigated. At 90 K, where the solvent is frozen, no quenching of the photosensitizer luminescence is observed for all the supramolecular systems. At 150 K, where the solvent is fluid, the results obtained were as follows. In the PTZ-$Ru(ttp)_2^{2+}$ dyad, neither quenching of the photosensitizer luminescence nor formation of oxidized donor are observed. In the DPAA-$Ru(ttp)_2^{2+}$ dyad, luminescence quenching and transient formation of the oxidized donor take place. For the $Ru(ttp)_2^{2+}$-MV^{2+} dyad, transient formation of the reduced acceptor is observed, but the lifetime of the photosensitizer luminescence *increases*, indicating that charge recombination leads back to the excited photosensitizer. The PTZ-$Ru(ttp)_2^{2+}$-MV^{2+} triad behaves as the $Ru(ttp)_2^{2+}$-MV^{2+} dyad. For the DPAA-$Ru(ttp)_2^{2+}$-MV^{2+} triad, strong luminescence quenching is observed, and transient absorption spectroscopy shows that charge separation is followed by a very fast charge recombination reaction ($\tau < 100$ ns). Thermodynamic and kinetic aspects of the photoinduced electron-transfer processes are discussed.

Introduction

Photoinduced electron-transfer processes in supramolecular species (dyads, triads, and tetrads) made of an organic or metallo-organic photosensitizer (P) covalently linked to electron acceptor (A) and/or electron donor (D) groups are currently the object of extensive investigations.[2-10] The role played by factors like energetics of the process, distance and relative orientation of the interacting partners, and influence of the connecting groups (spacers) and of the solvent has been investigated in great detail. In triads and tetrads the arrangement of the molecular components is designed to promote sequential electron-transfer steps, which lead to a charge-separated (CS) state where a fraction as large as possible of the light energy initially absorbed by the photosensitizer is stored, for a time as long as possible, as redox chemical energy. For a slow charge-recombination (CR) process, the final oxidized and reduced components must be sufficiently far apart and electronically "isolated" by suitable spacers.

Ru(II)-polypyridine complexes are, in principle, suitable photosensitizer components for such systems.[8-12] However, with the basic $(bpy)_3$ (bpy = 2,2'-bipyridine) ligand arrangement, the building up of supramolecular structures leads to systems where the components linked to the photosensitizer are relatively close to each other (cis-type configuration).[13] The geometry of $(trpy)_2$ complexes (trpy = 2,2':6',2''-terpyridine), on the contrary, offers the possibility to design supramolecular species in which the D and A components lie on opposite directions with respect to the photosensitizer (trans-type configuration).[14] In addition, $(trpy)_2$ complexes bearing substituents at the 4'-position do not lead to isomeric (enantio- and diastereomeric) mixtures contrary to their equivalent substituted $(bpy)_3$ systems. In other words, the bis(terpyridine)ruthenium(II) complexes synthesized and studied in the present paper are single chemical species. This is due to the fact that in each substituted trpy the anchoring point to the electroactive group belongs to the symmetry elements of the ligand and of the $(trpy)_2$ complex (two symmetry planes and C_2 axis). Furthermore, the interposition of aromatic rings (Figure 1) affords a very convenient way to increase the A-D separation distance.[15]

In this paper, we report the synthesis of some supramolecular systems (illustrated in Figure 1), which have been designed on the basis of the above ideas, and we describe their spectroscopic, photochemical, and electrochemical behavior. Any attempt to rationalize the results obtained with a supramolecular system can only be based on the identification of the molecular species (components) that constitute the system.[10] Such an identification process is always somewhat arbitrary and often can only be justified a posteriori. Figure 1 shows the ways in which we have "subdivided" the various supramolecular systems into molecular components and illustrates the abbreviations used;[16] the distance between the X and Y components is 21 Å.

Electrochemical and spectroscopic experiments have been employed to establish the thermodynamic aspects of photoinduced charge separation in the dyads and triads. Transient absorption spectra and quenching of the photosensitizer luminescence intensity and lifetime have been used to monitor electron-transfer processes and to obtain electron-transfer rate constants. Extended Hückel MO calculations have provided information on the extent of

(1) (a) Université Louis Pasteur. (b) Istituto FRAE-CNR. (c) Dipartimento di Chimica "G. Ciamician" dell' Università di Bologna.
(2) It would be impossible to give an exhaustive list of original papers on this subject. For recent reviews and articles of general interest, see refs 3-10.
(3) Oevering, H.; Paddon-Row, M. N.; Heppener, M.; Oliver, A. M.; Cotsaris, E.; Verhoeven, J. W.; Hush, N. S. *J. Am. Chem. Soc.* **1987**, *109*, 3258.
(4) Closs, G. L.; Miller, J. R. *Science* **1988**, *240*, 440.
(5) Connolly, J. S.; Bolton, J. R. In *Photoinduced Electron Transfer, Part D*; Fox, M. A., Chanon, M., Eds.; Elsevier: Amsterdam, 1988; p 303.
(6) Wasielewski, M. R. In *Photoinduced Electron Transfer, Part A*; Fox, M. A., Chanon, M., Eds.; Elsevier: 1988, p 161.
(7) Gust, D.; Moore, T. A. *Tetrahedron* **1989**, *45*, 4669-4903.
(8) Meyer, T. J. *Acc. Chem. Res.* **1989**, *22*, 163.
(9) Scandola, F.; Indelli, M. T.; Chiorboli, C.; Bignozzi, C. A. *Top. Curr. Chem.* **1990**, *158*, 73.
(10) Balzani, V.; Scandola, F. *Supramolecular Photochemistry*; Horwood: Chichester, U.K., 1990; Chapter 5.
(11) Juris, A.; Balzani, V.; Barigelletti, F.; Campagna, S.; Belser, P.; von Zelewsky, A. *Coord. Chem. Rev.* **1988**, *84*, 85.
(12) Balzani, V.; Barigelletti, F.; De Cola, L. *Top. Curr. Chem.* **1990**, *158*, 31.
(13) Danielson, E.; Elliot, C. M.; Merckert, J. W.; Meyer, T. J. *J. Am. Chem. Soc.* **1987**, *109*, 2519.
(14) Constable, E. C. *Adv. Inorg. Chem. Radiochem.* **1986**, *30*, 69.
(15) Collin, J.-P.; Guillerez, S.; Sauvage, J.-P. *J. Chem. Soc., Chem. Commun.* **1989**, 776.
(16) In covalently linked multicomponent systems there are nomenclature problems related to the fact that covalent linking implies more or less small modifications of the isolated molecular species. For example, 4'-*p*-tolyl-2,2':6',2''-terpyridine and its abbreviation ttp are right when used for the ligands of the isolated photosensitizer $Ru(ttp)_2^{2+}$ but are not correct when applied to the photosensitizer component of a dyad and triad. It is however preferable to maintain the same abbreviations for the free and covalently linked components in order to better understand the chemical parentage of the various systems investigated.

0020-1669/91/1330-4230$02.50/0

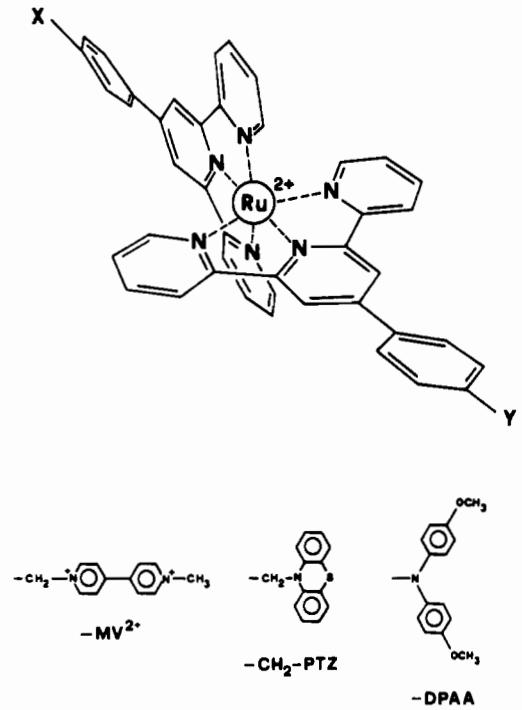

Figure 1. Illustration of the investigated systems and abbreviations used: X = $-CH_3$, Y = $-CH_3$, P photosensitizer, $Ru(ttp)_2^{2+}$; X = $-CH_3$, Y = $-MV^{2+}$ P–A photosensitizer–acceptor dyad, $Ru(ttp)_2^{2+}-MV^{2+}$; X = $-CH_2$–PTZ or –DPAA, Y = CH_3, D–P donor–photosensitizer dyads, PTZ–$Ru(ttp)_2^{2+}$ and DPAA–$Ru(ttp)_2^{2+}$; X = $-CH_2$–PTZ or –DPAA, Y = $-MV^{2+}$, D–P–A donor–photosensitizer–acceptor triads, PTZ–$Ru(ttp)_2^{2+}-MV^{2+}$ and DPAA–$Ru(ttp)_2^{2+}-MV^{2+}$.

electronic delocalization in trpy and ttp ligands.

Experimental Section

Instrumentation. ^1H NMR spectra were acquired on a Bruker WP200SY instrument. Chemical shifts are reported referenced to Me_4Si as an internal standard. Mass spectra were obtained by using VG ZAB-HF and Thomson THN 208 mass spectrometers. Melting points were determined on a Büchi SMP20 apparatus and were uncorrected. Elemental analyses of C, H, and N were performed by the Service de l'Institut de Chimie de Strasbourg.

Cyclic voltammetry was carried out on a Bruker EI310M potentiostat connected to a Ifelec 3802 XY recorder with a three-electrode system: either a Pt or GC electrode as working electrode, a Pt-wire coil as auxiliary electrode, and a sodium saturated calomel electrode (SSCE) as reference were used. The reference electrode was separated from the bulk of the solution by a glass tube fitted on the bottom with a fine porosity sintered glass and was immersed in a CH_3CN solution containing Bu_4NClO_4 (0.1 M). Experiments were carried out at 22 ● 1 °C in solutions previously degassed for 20 min with argon of high purity. Potentials are reported vs SSCE, the sweep rate was 200 mV s^{-1}, and the experimental uncertainty was ±20 mV.

Ground-state absorption, luminescence, and transient absorption experiments at the indicated temperatures were carried out in acetonitrile or in a mixture (hereafter called "nitrile") of freshly distilled propionitrile–butyronitrile (4:5 v/v). Dilute (10^{-4}–10^{-5} M) solutions of the samples were sealed under vacuum in 1-cm quartz cells after repeated freeze–pump–thaw cycles. The cells were placed inside a modified Thor C600 nitrogen flow cryostat, equipped with a Thor 3030 temperature controller. The absolute error on the temperature is estimated to be ±2 K.

The ground-state absorption spectra were recorded with either a Perkin-Elmer Lambda 5 or a Kontron Uvikon 860 spectrophotometer. Corrected emission spectra were obtained with a Spex Fuorolog-2 fluorimeter by using software supplied by the firm. The uncertainties on the reported measurements of emission maxima and relative luminescence intensities are estimated to be ±2 nm and ±20% respectively.

The luminescence lifetimes were measured by using Edimburgh 199 and Applied Photophysics single-photon counting instruments employing nitrogen or hydrogen excitation lamps (pulse width 2.5 and 1.5 ns, respectively; response time 0.2 ns) and equipped with an IBM or an Epson PC. Analyses of the decay profiles were performed by using either firm-supplied software or homemade programs based on least-squares iterative nonlinear procedures.[17]

Time-resolved absorption spectra and kinetics were detected by a laser flash photolysis apparatus based on a Nd:YAG laser (JK Lasers) with 20-ns pulse duration. The second harmonic (λ = 532 nm) was used for excitation. Samples with absorbance = 0.1–0.2 at the excitation wavelength were employed. The beam was focused to an area of 10 mm wide × 3 mm high. The light of a pulsed xenon arc lamp probed, at a right angle, a small volume of irradiated solution (2 mm deep × 3 mm high) in the first slice of the irradiated sample. A mask placed on the cell holder of the cryostat prevented extraneous light from reaching the analyzed area. The light transmitted by the sample was focused on a monochromator and detected with a resolution of 4 nm by a R936 photomultiplier. Sequence generation, lamp pulser, and automatic back-off were homemade. The energy used was approximately 10 mJ/pulse on the irradiated area. A Tektronix 468 digital storage oscilloscope or a Tektronix R7912 transient digitizer in conjunction with a Digital PDP 11/23 microcomputer were used to acquire and process the signals by standard iterative nonlinear procedures. For the transient absorption experiments, the instrument resolution time was 20 ns.

For the decay of the luminescence intensity and transient absorption, the goodness of the fit between the experimental points and the applied mathematical functions was judged on the basis of a reduced χ^2 close to unity and a regular distribution of the residuals along the time axis.[17] The estimated uncertainty on the lifetimes was ±10%.

Chemicals. High-purity commercial reagent grade products were used without purification, except tetrahydrofuran (THF), which was distilled from sodium–benzophenone. Sodium hydride (55–60% oil dispersion) was washed with hexane and then dried in vacuo prior to the reaction. The purification of all ruthenium complexes was performed on chromatography columns protected from light by aluminum foil. The compounds 1-methyl-4,4′-bipyridinium iodide,[18] dianisylphenylamine,[19] and 4-(N,N′-di-*p*-anisylamino)benzaldehide[20] were prepared according to literature procedures.

4′-*p*-Tolyl-2,2′:6′,2″-terpyridine (ttp). The synthesis of ttp was undertaken by following a method previously described,[21,22] with some modifications. A mixture of acetamide (183 g, 3.1 mol), ammonium acetate (118 g, 1.5 mol), *p*-tolylaldehyde (12.4 g, 103 mmol), and 2-acetylpyridine (25 g, 206 mmol) was refluxed for 2 h and cooled to 120 °C, and NaOH (90 g in 200 cm^3 of water) was added. After a further 2 h at 120 °C without stirring, the solution was cooled to room temperature. A brown solidified paste was separated, washed with water, and dissolved in acetic acid (60 cm^3). The hydrobromide salt was precipitated with 47% HBr (60 cm^3), filtered off, and dissolved in water (200 cm^3). The aqueous solution was made alkaline with KOH (pH 10). The suspension obtained was extracted with CH_2Cl_2 (3 × 200 cm^3). After evaporation of the solvent, the residue was recrystallized from ethanol (400 cm^3) to give white needles (11 g). At this stage, TLC (Al_2O_3, ether–hexane 1:1) and ^1H NMR revealed the presence of two compounds. The needles obtained were dissolved in an ethanol–dichloromethane mixture (1:1, 500 cm^3), and a Mohr salt aqueous solution (5.9 g in 100 cm^3) was added to give immediately a purple solution. An aqueous solution of KPF_6 (5.6 g in 50 cm^3) was added after evaporation of CH_2Cl_2. The precipitate was collected, redissolved in CH_3CN (100 cm^3) and washed with toluene (3 × 100 cm^3). Characterization of the isolated precipitate (elemental analysis, ^1H NMR, cyclic voltammetry) confirms the formula $Fe(ttp)_2(PF_6)_2$. ttp was liberated from the complex by oxidation of the iron(II) by H_2O_2 in alkaline medium following the procedure described by Constable et al.[23] (7.7 g, 23%): mp 174–176 °C; δ_H (CD_2Cl_2) 8.77 (2 H, s), 8.76–8.68 (4 H, m), 7.92 (2 H, td, J = 7.7 and 1.9 Hz), 7.84 (2 H, d, J = 8.2 Hz), 7.42–7.36 (4 H, m), 2.46 (3 H, s); m/z 323 ($C_{22}H_{17}N_3$ requires m/z 323.4). Anal. Calcd for $C_{22}H_{17}N_3$: C, 81.71; H, 5.30; N, 12.99. Found: C, 81.49; H, 5.29; N, 12.81.

The toluene extracts after evaporation yielded 3.0 g of a white product, which was analyzed as 6′-*p*-tolyl-2,2′:4′,2″-terpyridine (9%): mp 142 °C; δ_H (CD_2Cl_2) 8.98 (1 H, d, J = 1.5 Hz), 8.83–8.72 (2 H, m), 8.71 (1 H, d, J = 9 Hz), 8.51 (1 H, d, J = 1.5 Hz), 8.20 (2 H, d, J = 8.2 Hz), 8.07 (1 H, d, J = 8.9 Hz), 7.96–7.86 (2 H, m), 7.44–7.36 (4 H, m), 2.47 (3 H, s); m/z 323 ($C_{22}H_{17}N_3$ requires m/z 323.40). Anal. Calcd for $C_{22}H_{17}N_3$: C, 81.71; H, 5.30; N, 12.99. Found: C, 81.66; H, 5.39; N, 13.14.

(17) Bevington, P. R. *Data Reduction and Error Analysis for the Physical Sciences*; McGraw Hill: New York, 1969.
(18) Emmert, B.; Stawitz, J. *Ber. Dtsch. Chem. Ges.* **1923**, B, *56*, 83.
(19) Wieland, H. *Ber. Dtsch. Chem. Ges.* **1910**, *43*, 705.
(20) Baker, T. N.; Doherty, W. P.; Kelley, W. S.; Newmeyer, W.; Rogers, J. E.; Spalding, R. E.; Walter, R. I. *J. Org. Chem.* **1965**, *30*, 3714.
(21) Case, F. H.; Kaspen, T. J. *J. Am. Chem. Soc.* **1956**, *78*, 5842.
(22) Spahni, W.; Calzaferri, G. *Helv. Chim. Acta* **1984**, *67*, 450.
(23) Constable, E. C.; Ward, M. D.; Corr, S. *Inorg. Chim. Acta* **1988**, *141*, 201.

4′-(*p*-Bromomethylphenyl)-2,2′:6′,2″-terpyridine (ttp–Br). The procedure was identical with that described by Calzaferri[22] with the exception that the solvent used was benzene instead of CCl_4. The yield was improved from 72 to 87%. Characterization data for ttp–Br: mp 175–176 °C; δ_H (CD_2Cl_2) 8.79 (2 H, s), 8.76–8.69 (4 H, m), 7.98–7.89 (4 H, m), 7.61 (2 H, d, J = 6.5 Hz), 7.41 (2 H, ddd, J = 7.5, 4.8, 1.3 Hz). Anal. Calcd for $C_{22}H_{16}BrN_3$: C, 65.68; H, 4.01; N, 10.44. Found: C, 65.42; H, 3.91; N, 10.49.

4′-[*p*-(1-Methyl-4,4′-bipyridinium-1′-yl)methylphenyl]-2,2′:6′,2″-terpyridine Dinitrate (ttp–MV^{2+},2NO_3^-). A mixture of ttp–Br (0.5 g, 1.24 mmol) and 1 methyl-4,4′-bipyridinium iodide (0.8 g, 2.7 mmol)[18] in absolute ethanol (100 cm^3) was refluxed for 3 days under argon. After removal of the solvent, the residue was washed with warm toluene (3 × 50 cm^3) and recrystallized twice from a methanol–ethanol mixture (4:6). The chloride or nitrate salts were obtained by passage over anionic exchange column (Dowex 1X-100). The hexafluorophosphate salt was obtained by anionic exchange with NH_4PF_6 (0.48 g, 50%): δ_H (CD_3CN) 9.04 (2 H, d, J = 7.0 Hz), 8.86 (2 H, d, J = 6.8 Hz), 8.77 (2 H, s), 8.76–8.69 (4 H, m), 8.43 (2 H, d, J = 7 Hz), 8.40 (2 H, d, J = 6.9 Hz), 8.07–7.94 (4 H, m), 7.72 (2 H, d, J = 8.3 Hz), 7.53–7.46 (2 H, m), 5.94 (2 H, s), 4.42 (3 H, s).

4′-(*p*-Phenothiazine-*N*-ylmethylphenyl)-2,2′:6′,2″-terpyridine (ttp–PTZ). Phenothiazine (2.00 g, 10 mmol) in anhydrous THF (30 cm^3) was added to NaH (0.43 g, 18 mmol) under argon. The suspension was heated to 50 °C for 2 h. After filtration, the residue was washed with THF (2 × 5 cm^3), and the orange filtrate was added to a THF (30 cm^3) solution of ttp–Br. The mixture was stirred at room temperature overnight and then quenched with methanol (6 cm^3). The solvents were removed, and the residue was washed with water (3 × 75 cm^3). It was purified by chromatography (alumina–CH_2Cl_2) to give a white powder (2.17 g, 84%): mp 181–182 °C; δ_H (CD_2Cl_2) 8.74 (2 H, s), 8.72–8.65 (4 H, m), 7.94–7.84 (4 H, m), 7.50 (2 H, d, J = 8.4 Hz), 7.53–7.33 (2 H, m), 7.15–6.71 (8 H, m), 5.21 (2 H, s); m/z 520 ($C_{34}H_{24}N_4S$ requires m/z 520.6). Anal. Calcd for $C_{34}H_{24}N_4S$: C, 78.43; H, 4.65; N, 10.76. Found: C, 78.62; H, 4.83; N, 10.50.

4-(*N*,*N*-Di-*p*-anisylamino)benzaldehyde.[20] $POCl_3$ (2.0 g, 13.1 mmol) was added dropwise at 0 °C to anhydrous DMF (3.63 g, 50 mmol). The solution was treated at 20 °C by dianisylphenylamine[19] (4.00 g, 13.1 mmol) in small amounts. The resulting suspension was refluxed for 2 h. Water (50 cm^3) was added to the cooled reaction mixture, which was extracted by CH_2Cl_2 (3 × 100 cm^3). The solvent was evaporated and the residue purified by silica gel column chromatography (CH_2Cl_2) to give a yellow solid (3.1 g, 71%): mp 101–102 °C; δ_H (CD_2Cl_2) 9.72 (1 H, s), 7.60 (2 H, d, J = 8.9 Hz), 7.14 (4 H, d, J = 9 Hz), 6.90 (4 H, d, J = 9 Hz), 6.82 (2 H, d, J = 8.8 Hz), 3.80 (6 H, s).

4′-[(*p*-*N*,*N*-Di-*p*-anisylamino)phenyl]-2,2′:6′,2″-terpyridine (ttp–DPAA). The aldehyde used was 4-(*N*,*N*-di-*p*-anisylamino)benzaldehyde. The synthetic method was analogous to the one described for ttp except that the product was purified by column chromatography (alumina; 6.5/3.5 hexane–ether; yield 23%): mp 194 °C; δ_H (CD_2Cl_2): 8.70 (2 H, s), 8.72–8.65 (4 H, m), 7.89 (2 H, td, J = 7.7 and 1.9 Hz), 7.74 (2 H, d, J = 8.8 Hz), 7.39–7.32 (2 H, m), 7.12 (4 H, d, J = 9.1 Hz), 7.00 (2 H, d, J = 8.9 Hz), 6.88 (4 H, d, J = 9.0 Hz), 3.80 (6 H, s); FAB-MS (nitrobenzyl alcohol matrix) m/z 537.2 ($C_{35}H_{28}N_4O_2$ + 1 requires m/z 537.44). Anal. Calcd for $C_{35}H_{28}N_4O_2$: C, 78.34; H, 5.26; N, 10.44. Found: C, 78.20; H, 5.29; N, 10.27.

Ru(ttp)Cl_3 and Ru(ttp)$_2$(PF_6)$_2$. These two compounds were obtained by following methods similar to those previously described for trpy.[24-26] Characterization data for Ru(ttp)$_2$(PF_6) (yield 75%): δ_H (CD_3CN) 8.99 (4 H, s), 8.64 (4 H, d, J = 8.3 Hz), 8.11 (4 H, d, J = 8.3 Hz), 7.94 (4 H, td, J = 7.9 and 1.4 Hz), 7.58 (4 H, d, J = 7.9 Hz), 7.43 (4 H, dd, J = 5.5 and 0.9 Hz), 7.21–7.14 (4 H, m), 2.54 (6 H, s). Anal. Calcd for $C_{44}H_{34}N_6P_2F_{12}Ru$: C, 50.92; H, 3.30; N, 8.10. Found: C, 50.68; H, 3.47; N, 8.06.

[PTZ–Ru(ttp)$_2$])(PF_6)$_2$ (See Figure 1). A suspension of Ru(ttp)Cl_3 (0.18 g, 0.34 mmol) and ttp–PTZ (0.17 g, 0.34 mmol) in an ethanol–triethylamine–water mixture (35:5:3) were refluxed under argon for 1 h. After cooling and filtration, the filtrate obtained was added to an aqueous solution of KPF_6 (0.2 g in 150 cm^3 of water). The precipitate formed was washed successively with water (200 cm^3), toluene (100 cm^3), and ether (100 cm^3). The product was purified by silica gel chromatography, eluting with CH_3CN–aqueous solution of KNO_3 mixture (95:5, KNO_3 1.5 × 10^{-2} M) (yield 0.021 g, 5%): δ_H (CD_3CN) 8.99 (2 H, s), 8.98 (2 H, s), 8.63 (4 H, d, J = 8.2 Hz), 8.17 (2 H, d, J = 8.4 Hz), 8.11 (2 H, d, J = 8.1 Hz), 7.93 (4 H, t, J = 7.9 Hz), 7.77 (2 H, d, J = 8.1 Hz), 7.58 (2 H, d, J = 8.0 Hz), 7.43–7.39 (4 H, m), 7.24–6.92 (12 H, m), 5.34 (2 H, s), 2.54 (3 H, s).

[DPAA–Ru(ttp)$_2$])(PF_6)$_2$ (See Figure 1). The procedure was identical with that for [PTZ–Ru(ttp)$_2$])(PF_6)$_2$ with the substitution of DPAA–ttp to give the product (yield 37%): δ_H (CD_3CN) 8.98 (2 H, s), 8.92 (2 H, s), 8.65–8.69 (4 H, m), 8.11 (2 H, d, J = 8.2 Hz), 8.03 (2 H, d, J = 8.9 Hz), 7.97–7.92 (4 H, m), 7.58 (2 H, d, J = 8.1 Hz), 7.46–7.38 (4 H, m), 7.24 (4 H, d, J = 9 Hz), 7.01 (4 H, d, J = 9 Hz), 7.26–6.99 (6 H, s), 3.83 (6 H, s), 2.54 (3 H, s). Anal. Calcd for $C_{57}H_{45}N_7O_2P_2F_{12}Ru$: C, 54.72; H, 3.62; N, 7.84. Found: C, 54.78; H, 4.12; N, 7.26.

[Ru(ttp)$_2$–MV](PF$_6$)$_4$ (See Figure 1). A "ruthenium blue" solution[27] (0.41 mmol of Ru in 70 cm^3 of methanol) was added under argon to a homogeneous solution of equimolar amounts of ttp and ttp–MV^{2+}, 2Cl^- in ethanol (50 cm^3). The reaction mixture was stirred under reflux for 18 h. After cooling and filtration, the orange-red filtrate was treated by an aqueous solution of KPF_6 (1 g in 150 cm^3 of water). The precipitate obtained was washed with water (150 cm^3) and the mixture of three ruthenium complexes was separated by silica gel chromatography. Elution with KNO_3 in a CH_3CN–water mixture (85:15–60:40; KNO_3 0.08–0.5 M) gave Ru(ttp)$_2$(PF_6)$_2$ (0.103 g, 26%), [Ru(ttp)$_2$–MV](PF$_6$)$_4$ (0.14 g, 25%), and Ru(ttp–MV^{2+})$_2$(PF_6)$_4$ (0.078 g, 11%).

Characterization data for [Ru(ttp)$_2$–MV](PF$_6$)$_4$: δ_H (CD_3CN): 9.14 (2 H, d, J = 7.1 Hz), 9.02 (4 H, s), 8.91 (2 H, d, J = 6.8 Hz), 8.67 (4 H, d, J = 8.2 Hz), 8.52 (2 H, d, J = 7.0 Hz), 8.44 (2 H, d, J = 6.8 Hz), 8.34 (2 H, d, J = 8.4 Hz), 8.13 (2 H, d, J = 8.2 Hz), 8.01–7.93 (4 H, m), 7.87 (2 H, d, J = 8.3 Hz), 7.60 (2 H, d, J = 8.1 Hz), 7.48–7.42 (4 H, m), 7.25–7.15 (4 H, m); 6.04 (2 H, s); 4.44 (3 H, s), 2.56 (3 H, s). Anal. Calcd for $C_{55}H_{44}N_8P_4F_{24}Ru$: C, 44.10; H, 2.96; N, 7.48. Found: C, 43.86; H, 3.44; N, 7.46.

[PTZ–Ru(ttp)$_2$–MV](PF$_6$)$_4$ and [DPAA–Ru(ttp)$_2$–MV](PF$_6$)$_4$ (See Figure 1). These triads were obtained in the manner described for [Ru(ttp)$_2$–MV](PF$_6$)$_4$. Characterization data for [PTZ–Ru(ttp)$_2$–MV](PF$_6$)$_4$ (yield 5%): δ_H (CD_3CN) 9.13 (2 H, d, J = 6.9 Hz), 9.00 (2 H, s), 8.99 (2 H, s), 8.88 (2 H, d, J = 6.7 Hz), 8.66 (2 H, d, J = 3.5 Hz), 8.62 (2 H, d, J = 3.6 Hz), 8.50 (2 H, d, J = 6.9 Hz), 8.42 (2 H, d, J = 6.8 Hz), 8.32 (2 H, d, J = 8.3 Hz), 8.18 (2 H, d, J = 8.3 Hz), 7.94 (4 H, t, J = 7.9 Hz), 7.85 (2 H, d, J = 8.2 Hz), 7.77 (2 H, d, J = 8.1 Hz), 7.44–7.39 (4 H, m), 7.24–6.92 (12 H, m), 6.02 (2 H, s), 5.34 (2 H, s), 4.42 (2 H, s); FAB-MS (nitrobenzyl alcohol matrix) m/z 1550.1 [PTZ–Ru(ttp)$_2$–MV](PF$_6$)$_3^+$ requires m/z 1550). Characterization data for [DPAA–Ru(tpp)$_2$–MV](PF$_6$)$_4$ (yield 8%): δ_H (CD_3CN) 9.11 (2 H, d, J = 6.9 Hz), 8.99 (2 H, s), 8.93 (2 H, s), 8.88 (2 H, d, J = 6.7 Hz), 8.66–8.59 (4 H, m), 8.49 (2 H, d, J = 6.9 Hz), 8.41 (2 H, d, J = 6.4 Hz), 8.32 (2 H, d, J = 8.3 Hz); 8.04 (2 H, d, J = 8.9 Hz), 7.96–7.88 (4 H, m), 7.84 (2 H, d, J = 8.2 Hz), 7.46 (2 H, d, J = 4.7 Hz), 7.38 (2 H, d, J = 4.9 Hz), 7.24 (4 H, d, J = 8.9 Hz), 7.01 (4 H, d, J = 9.1 Hz), 7.25–7.00 (6 H, m), 6.01 (2 H, s), 4.42 (3 H, s), 3.83 (6 H s); FAB-MS (nitrobenzyl alcohol matrix) m/z 1566.1 [DPAA–Ru(ttp)$_2$–MV](PF$_6$)$_3^+$ requires m/z 1566].

Results

Synthesis of the Ligands. The synthesis of 2,2′:6′,2″-terpyridines covalently linked to either electron-acceptor or electron-donor groups has been carried out from 4′-tolyl-2,2′:6′,2″-terpyridine (ttp), which contains a rigid spacer easily convertible to the reactive bromomethyl derivative (ttp–Br). In order to obtain large amounts of the terpyridine precursor, the one-pot Hantzsch synthesis, developed by Case[21] and later by Calzaferri,[22] was selected. Contrary to previously published work,[22] the purification of ttp by crystallization in ethanol or chromatography (alumina or silica gel) proved to be ineffective. In fact, two terpyridine isomers were isolated and characterized. These two isomers can be obtained following a 1,2 or 1,4 Michael addition on the unsaturated ketone intermediate produced by the condensation of the aromatic aldehyde and 2-acetylpyridine (Scheme I).

The separation of the terdentate ttp ligand and the sterically hindered bidentate ligand 6′-t-2,2′:4′,2″-tp was readily performed by formation of the highly stable Fe(ttp)$_2^{2+}$ complex as previously described.[23] The iron(II) complex, treated with H_2O_2 in alkaline solution, yields the free ttp ligand in good yield.

ttp–PTZ was made by the reaction of ttp–Br with the sodium salt of the phenothiazine anion. ttp–MV^{2+} was obtained from ttp–Br and (*N*-methyl-4-pyridiniumyl)pyridinium iodide. ttp–DPAA was synthesized in the same straightforward way as ttp

(24) Klassen, D. M.; Hudson, C. W.; Shaddix, E. L. *Inorg. Chem.* **1975**, *14*, 2733.
(25) Belser, P.; Von Zelewsky, A. *Helv. Chim. Acta* **1980**, *63*, 1675.
(26) Sullivan, B. P.; Calvert, J. M.; Meyer, T. J. *Inorg. Chem.* **1980**, *19*, 1404.
(27) Rose, D.; Wilkinson, G. *J. Chem. Soc. A* **1970**, 1791.

Table I. Electrochemical Potentials[a] and Their Assignments

	Ru^{3+}/Ru^{2+}	$DPAA^{+/0}$	$PTZ^{+/0}$	$MV^{2+/+}$	ttp/ttp^{-}[b]
$Ru(ttp)_2^{2+}$	+1.25				−1.24
MV^{2+}				−0.44[c]	
MePTZ			+0.74[d]		
MeDPAA		+0.65[e]			
$Ru(ttp)_2^{2+}$–MV^{2+}	+1.27			−0.36	−1.21
PTZ–$Ru(ttp)_2^{2+}$	+1.27		+0.79		−1.23
DPAA–$Ru(ttp)_2^{2+}$	+1.27	+0.77			−1.26
PTZ-$Ru(ttp)_2^{2+}$–MV^{2+}	+1.25		+0.76	−0.39	−1.24
DPAA-$Ru(ttp)_2^{2+}$–MV^{2+}	+1.26	+0.75		−0.40	−1.26

[a] Acetonitrile solution, 298 K; $E_{1/2}$ values in V, vs SSCE. [b] The reduction wave of the second ttp ligand occurs at more negative potentials. [c] $E_{1/2}$ = −0.40 V vs Ag/AgCl;[28] the reduction potential for the ttp–MV^{2+} moiety is −0.36 V. [d] $E_{1/2}$ = +0.40 V vs Ag/Ag^{+};[29] the reduction potential for the ttp–PTZ^{+} moiety is +0.79 V. [e] Methyldi-*p*-anisylamine;[30] the reduction potential for the ttp–$DPAA^{+}$ moiety is +0.74 V.

Scheme I

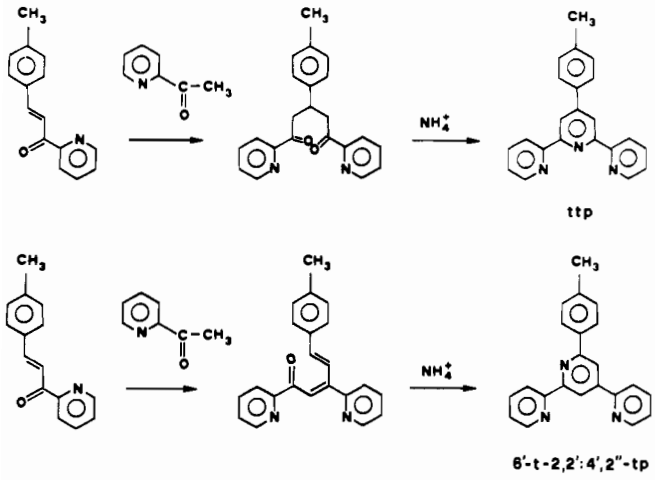

by condensation of 2 equiv of 2-acetylpyridine with 1 equiv of (bis(*p*-methoxyphenyl)amino)benzaldehyde. The latter compound was obtained by formylation of bis(*p*-methoxyphenyl)phenylamine in classical fashion.[20]

Synthesis of the Ruthenium Complexes. The reference complex $Ru(ttp)_2(PF_6)_2$ was prepared in good yield from $RuCl_3 \cdot 3H_2O$ and ttp in ethylene glycol under reflux, as for many other polypyridine complexes of ruthenium(II).[24,25] This procedure cannot be applied to ligands bearing easily oxidized or reduced chemical groups. For the dyads PTZ–$Ru(ttp)_2^{2+}$ and DPAA–$Ru(ttp)_2^{2+}$, a better, but still low yield was obtained in two steps: (i) preparation of $Ru(ttp)Cl_3$ as for $Ru(trpy)Cl_3$[26] and (ii) reaction of the functionalized terpyridine with $Ru(ttp)Cl_3$ in ethanol under reflux in presence of a mild reducing agent. In the case of the dyad and triads bearing the ttp–MV^{2+} ligand, the most suitable preparation consisted of a statistical method based on the reaction of 1 equiv of each different ligand with 1 equiv of a ruthenium(II) precursor ("ruthenium blue solution").[27]

The purity of the highly colored complexes was checked carefully by TLC on SiO_2 (CH_3CN–H_2O–KNO_3 as eluent) and by 200-MHz ^1H NMR.

Electrochemistry. The electrochemical properties of the investigated systems at room temperature in acetonitrile solution are listed in Table I. The isolated $Ru(ttp)_2^{2+}$ photosensitizer shows a reversible oxidation wave at +1.25 V and a reversible reduction wave at −1.24 V. Comparison with results of extended investigations performed on complexes of the Ru(II)–polypyridine family[11] allows us to assign the oxidation wave to a metal-centered process and the reduction wave to the one-electron reduction of a ligand. The well-known reduction wave of MV^{2+} is reversible, and this is also the case for the first oxidation wave of PTZ and phenyldi-*p*-anisylamine, MeDPAA, which may be considered a reference compound for –DPAA. The reduction of the second ttp ligand (−1.47 V), the second reduction of MV^{2+}, and the second oxidations of PTZ and MeDPAA are not relevant to our discussion. The electrochemical waves of the dyads and triads can

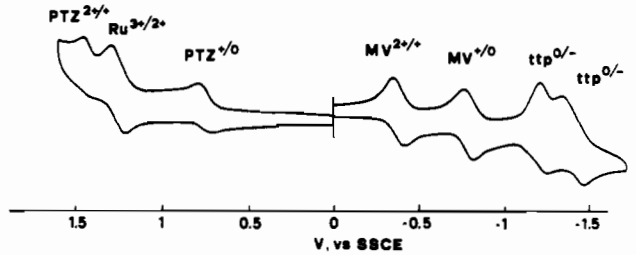

Figure 2. Cyclic voltammogram for the PTZ–P–MV^{2+} triad.

Table II. Ground State Absorption Maxima[a]

	λ_{max}, nm (ϵ, M^{-1} cm^{-1})		
$Ru(ttp)_2^{2+}$	284 (68 000)	310 (76 000)	490 (28 000)
$Ru(ttp)_2^{2+}$–MV^{2+}	285 (98 000)	311 (79 000)	491 (32 000)
PTZ–$Ru(ttp)_2^{2+}$	285 (75 000)	310 (84 000)	490 (31 000)
DPAA–$Ru(ttp)_2^{2+}$	284 (63 000)	310 (81 000)	502 (39 000)
PTZ–$Ru(ttp)_2^{2+}$–MV^{2+}	285 (112 000)	310 (83 000)	491 (32 000)
DPAA–$Ru(ttp)_2^{2+}$–MV^{2+}	283 (83 000)	310 (77 000)	504 (43 000)
$Ru(trpy)_2^{2+}$[b]			470 (16 100)

[a] Acetonitrile solutions, 298 K. [b] Methanol solution.[31]

easily be assigned by comparison with the waves observed for the isolated components (Table I). The cyclic voltammogram for the [PTZ–$Ru(ttp)_2$–MV]$^{4+}$ triad is presented in Figure 2. The energies of the various charge-separated states in the examined dyads and triads can be estimated from the data of Table I. The values so obtained, however, are not the exact energy values of the various levels in the photochemical experiments because of the different solvent and temperature conditions (vide infra).

Ground-State Absorption Spectra. The absorption spectrum of $Ru(ttp)_2^{2+}$ is characterized by intense bands in the UV and visible regions (Table II). The bands centered at about 284 and 310 nm correspond to ligand-centered (^{1}LC) transitions, while those in the visible region correspond to metal-to-ligand charge-transfer transitions (^{1}MLCT, $Ru^{2+} \rightarrow$ ttp).[11,31,32] The latter type of transitions can be described as electron promotion from metal-centered d orbitals to unfilled ligand-centered π^* orbitals. The D and A components do not absorb in the visible region. Inspection of Table II reveals that the energy and the intensity of the MLCT transitions are hardly affected by the attached MV^{2+} and PTZ groups. When D = DPAA, the energy and intensity of the ^{1}MLCT band show some change with respect to the isolated photosensitizer and the other systems. The room-temperature absorption spectrum of the DPAA–$Ru(ttp)_2^{2+}$–MV^{2+} triad is shown in Figure 3.

(28) Hünig, S.; Grass, J.; Schenk, W. *Liebigs Ann. Chem.* **1973**, 324.
(29) Billon, J.-P. *Ann. Chim.* **1962**, *7*, 183.
(30) Seo, E. T.; Nelson, R. F.; Fritsch, J. M.; Marcoux, L. S.; Leedy, D. W.; Adams, R. N. *J. Am. Chem. Soc.* **1966**, *88*, 3498.
(31) Stone, M. L.; Crosby, G. A. *Chem. Phys. Lett.* **1981**, *79*, 169.
(32) Hecker, K. R.; Gushurst, A. K. I.; McMillin, D. R. *Inorg. Chem.* **1991**, *30*, 538.

Table III. Luminescence Data[a]

	90 K			150 K			200 K		
	λ_{max}, nm	τ, μs	I^b	λ_{max}, nm	τ, μs	I^b	λ_{max}, nm	τ, μs	I^b
$Ru(ttp)_2^{2+}$	628	9.1	100	648	2.3	21	647	0.05	0.6
$Ru(ttp)_2^{2+}$–MV^{2+}	634	9.5	66	661	4.2	16	664	0.67	1.3
PTZ–$Ru(ttp)_2^{2+}$	629	9.5	80	649	2.6	22	648	0.08	0.7
DPAA–$Ru(ttp)_2^{2+}$	656	13.9	128	678	0.4[c]	3	676	0.04	0.2
PTZ–$Ru(ttp)_2^{2+}$–MV^{2+}	632	9.5	96	658	3.7	26	660	0.66	1.7
DPAA–$Ru(ttp)_2^{2+}$–MV^{2+}	656	13.4	88	675	0.1[c]	<1	*d*	*d*	*d*
$Ru(trpy)_2^{2+}$[e]	598	11.0							

[a] Nitrile solutions; uncertainties ±10% on lifetimes, ±20% on intensities; excitation performed at 490 or 505 nm. [b] Relative intensity. [c] A minor (~10%) long-lived (microsecond time scale) component is also present. [d] No emission observed. [e] MeOH–EtOH (4:1 v/v) 77 K.[31]

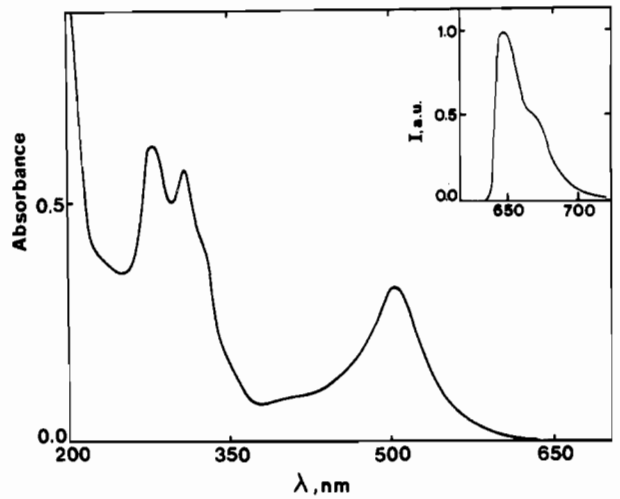

Figure 3. Absorption and (inset) emission spectra (77 K) of the DPAA–P–MV^{2+} triad.

In order to monitor the effect of decreasing temperature on the MLCT bands, absorption spectra were also obtained in propionitrile–butyronitrile solvent in the temperature range between 90 and 298 K. While the energy position of the band maximum did not show any change, the intensity of the band progressively increased for $T < 140$ K (+20% at 90 K), as expected because of solvent contraction.

Luminescence Properties. The photosensitizer, the dyads, and the triads do not emit at room temperature. The characteristic ^{3}CT luminescence of the photosensitizer, however, can be observed at lower temperature for both the isolated photosensitizer and the supramolecular species. This is the only type of luminescent emission that can be observed in all our systems.[33] Luminescence band maxima and lifetimes obtained at 90 K, where the propionitrile–butyronitrile solvent is frozen,[36] and at 150 and 200 K, where the solvent is fluid, are reported in Table III. The luminescence spectrum of the DPAA–$Ru(ttp)_2^{2+}$–MV^{2+} triad at 90 K is displayed in the inset of Figure 3.

From Table III one can see that at 90 K the band maxima for the photosensitizer P, the P–MV^{2+} and PTZ–P dyads, and the PTZ–P–MV^{2+} triads are in the range 628–634 nm. On the other hand, the systems containing DPAA exhibit band maxima centered at 656 nm. Similar differences between band maxima for the two types of systems are found at 150 and 200 K (Table III).

For all the dyads and triads examined, the luminescence measurements in frozen matrix at 90 K indicate little or no quenching of the luminescence intensity with respect to the isolated photosensitizer and comparable luminescence lifetimes are observed.

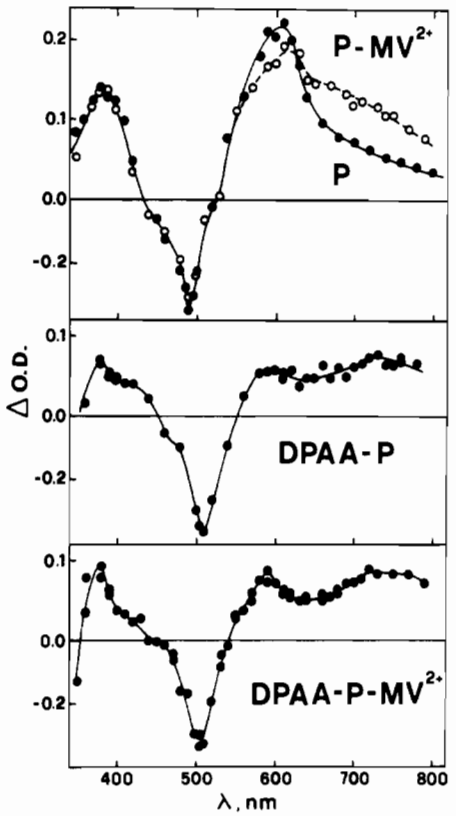

Figure 4. Transient difference absorption spectra, taken at 150 K at the end of the 20-ns laser pulse, for the photosensitizer P, the P–MV^{2+} and DPAA–P dyads, and the DPAA–P–MV^{2+} triad.

At 150 K the luminescence intensity of the isolated photosensitizer reduces to 21% of that obtained at 90 K, and a roughly parallel decrease in the luminescence lifetime is observed. A further, strong decrease of the luminescence intensity and lifetime occurs when one is going to 200 K.

A general decrease in the luminescence intensity and lifetime with increasing temperature is also observed for the dyads and triads, but a comparison with the data obtained for the isolated photosensitizer (Table III) indicates important differences for the various supramolecular species. The behavior of the PTZ–P dyad substantially parallels that of the isolated photosensitizer. For the DPAA–P dyad, in going from 90 to 150 K there is a strong intensity and lifetime quenching compared to the isolated P. For the P–MV^{2+} dyad increasing temperature causes a decrease in the luminescence intensity which roughly parallels that of the isolated photosensitizer, whereas the luminescence lifetime is considerably *less* quenched. The PTZ–P–MV^{2+} triad behaves essentially as the P–MV^{2+} dyad, whereas a very strong quenching effect is apparent with increasing temperature for the DPAA–P–MV^{2+} triad. It should also be noticed that while in all cases the decay is exponential, at 150 K the DPAA–P dyad and the

(33) Luminescence originating from charge recombination can sometimes be observed for chromophore-quencher systems.[34,35]
(34) Sullivan, B. P.; Abruna, H.; Finklea, H. O.; Salmon, D. J.; Nagle, J. K.; Meyer, T. J.; Sprintschnik, H. *Chem. Phys. Lett.* **1978**, *58*, 389.
(35) Oevering, H.; Verhoeven, J. W.; Paddon-Row, M. N.; Warman, J. M. *Tetrahedron* **1989**, *45*, 4751.
(36) Barigelletti, F.; Belser, P.; Von Zelewsky, A.; Juris, A.; Balzani, V. *J. Phys. Chem.* **1985**, *89*, 3680.

DPAA–P–MV^{2+} triad exhibit a two-exponential decay, with a major (90%) short-lived component and a minor (10%) long-lived one.

Transient Absorption Spectra. Laser flash-photolysis experiments were performed at 150 and 200 K in propionitrile–butyronitrile solvent. Transient absorption spectra were recorded immediately after the 20-ns excitation pulse, and their decay was monitored at several wavelengths. The transient absorption spectra obtained at 150 K for the photosensitizer P, the P–MV^{2+} and DPAA–P dyads, and the DPAA–P–MV^{2+} triads are shown in Figure 4.

The transient spectrum for the isolated photosensitizer showed positive absorptions at 390 and 600 nm, which, by analogy with the behavior of $Ru(bpy)_3^{2+}$,[11] can be ascribed to the ttp^- species present in the ^{3}MLCT excited state. A bleaching in the 430–520-nm region, corresponding to the disappearance of the ground-state MLCT band, was also observed. At 150 K, the transient absorption bands decayed following an exponential law with $\tau = 2.0$ μs, at both 390 and 600 nm, and the same lifetime was obtained for the recovery of the ground-state absorption, monitored at 490 nm. For the P–MV^{2+} dyad, the transient spectrum was quite similar to that of P alone, except for an intense shoulder at 650–750 nm, whose formation is complete within 30 ns after the end of the laser pulse. Since the absorption band of MV^+ ($\lambda_{max} = 600$ nm) is still relatively intense ($\epsilon \sim 3000$ M^{-1} cm^{-1} at $\lambda = 700$ nm),[37] the formation of this shoulder is ascribed to electron transfer from *P to MV^{2+}. No quantization of the charge-transfer yield is possible due to the poor separation of the ttp^- and MV^+ absorption spectra. The transient spectrum, detected at $t = 30$ ns after the end of the laser pulse, decayed exponentially with $\tau = 4.0$ μs at 380, 600, and 700 nm. The same lifetime value was obtained for the recovery of the ground-state absorption.

The transient absorption spectrum of the PTZ–$Ru(ttp)_2^{2+}$ dyad did not show any sizable change with respect to that of $Ru(ttp)_2^{2+}$; the decay of the spectrum followed an exponential law with $\tau = 2.9$ μs.

For the DPAA–P dyad, the transient difference spectrum (Figure 4) showed a bleaching comparable to that observed for P and P–MV^{2+} as well as a comparable absorption at 380 nm (after correction for ground-state absorption), whereas the band at 600 nm was less intense and broader. Furthermore a broad absorption band, present in the 700–800-nm region, is consistent with formation of $DPAA^+$, since ttp–$DPAA^+$ (obtained by electrochemical oxidation of ttp–DPAA) showed a maximum at $\lambda = 740$ nm. However, the transient absorption spectrum in the 600–800-nm region is much broader and weaker than expected from the sum of the $DPAA^+$ and P^- component spectra. The transient bands decayed exponentially with $\tau = 450$ ns.

The PTZ–$Ru(ttp)_2^{2+}$–MV^{2+} triad showed transient spectral features and a lifetime identical with those reported above for the $Ru(ttp)_2^{2+}$–MV^{2+} dyad.

The transient difference spectrum of the DPAA–P–MV^{2+} triad, Figure 4, is quite similar to that of the DPAA–P dyad. The transient spectrum detected at the end of the 20-ns laser pulse decayed exponentially with $\tau = 100$ ns at 380, 600, and 760 nm, and the same value was obtained for the recovery of the ground-state absorption at 505 nm.

Discussion

Photoinduced charge-separation processes in covalently linked supramolecular systems constituted by an octahedral metal complex (photosensitizer) and reductive and/or oxidative components (quenchers) have been investigated by Cooley et al.[38] and, in particular, by Meyer and co-workers.[8,13,34,39–44] Our triads are similar to the one studied by Meyer, Elliot, and co-workers,[13] where $Ru(bpy)_3^{2+}$ is covalently linked to bipiridinium and PTZ components by methylene spacers. The geometry of our system is better defined because of the trans-type arrangement of the oxidative and reductive quenchers made possible by the $Ru(ttp)_2^{2+}$ photosensitizer (Figure 1).

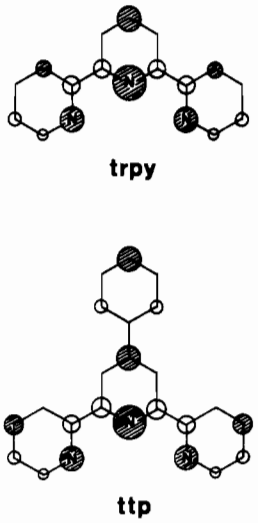

Figure 5. Representation of the LUMO of the trpy and ttp ligands.

Properties of the Isolated Photosensitizer. The $Ru(ttp)_2^{2+}$ photosensitizer is a metal complex that can be satisfactorily treated by a "localized" molecular orbital approach. In other words, it is possible (and meaningful) to distinguish metal-centered, ligand-centered, and charge-transfer excited states, as well as ligand-localized one-electron-reduction and metal-localized one-electron-oxidation processes.[11]

Visible-light absorption in the $Ru(ttp)_2^{2+}$ chromophore leads to population of a Ru → ttp ^{1}CT state that corresponds to the promotion of an electron from a metal-centered d orbital to the lowest unoccupied π^* molecular orbital (LUMO) of the ligand. According to current models for metal-to-ligand CT transitions,[35,44] the energy and intensity of the CT absorption band are related to (i) energy separation and extent of mixing of the involved metal-centered d and ligand-centered π^* orbitals and (ii) the average separation of the electron promoted into the ligand and the hole left on the metal center. A prominent contribution to the metal–ligand orbital mixing is provided by the atomic orbitals on the N coordinating positions.

Extended Hückel calculations show that the LUMO of the smaller trpy ligand and that of ttp (with the additional phenyl group taken coplanar to the trpy "core") lie very close in energy (−9.85 and −9.88 eV, respectively). Figure 5 shows the MO shapes in terms of C and N atomic contributions to the LUMO of the trpy and ttp ligands. For a $Ru(trpy)_2^{2+}$ type chromophore, one sees that symmetry allowed optical transitions only occur along the direction connecting the metal and the central N of the ligand.[45] As revealed by the results of Figure 5, the atomic contribution of the central N to the LUMO is quite similar for the trpy and ttp cases, while the promoted electron should be moved over a larger distance in the latter case. On the basis of the calculated properties for trpy and ttp, similar energies for the

(37) Venturi, M.; Mulazzani, G. Q.; Hoffman, M. Z. *Radiat. Phys. Chem.* **1984**, *23*, 229.
(38) Cooley, L. F.; Headford, C. E. L.; Elliot, C. M.; Kelly, D. F. *J. Am. Chem. Soc.* **1988**, *110*, 6673.
(39) Westmoreland, T. D.; Le Bozec, H.; Murray, R. W.; Meyer, T. J. *J. Am. Chem. Soc.* **1983**, *105*, 5952.
(40) Chen, P.; Westmoreland, T. D.; Danielson, E.; Schanze, K. S.; Anthon, D.; Neveux, P. E.; Meyer, T. J. *Inorg. Chem.* **1987**, *26*, 1116.
(41) Chen, P.; Duesing, R.; Tapolsky, G.; Meyer, T. J. *J. Am. Chem. Soc.* **1989**, *111*, 8305.
(42) Duesing, R.; Tapolsky, G.; Meyer, T. J. *J. Am. Chem. Soc.* **1990**, *112*, 5378.
(43) Chen, P.; Danielson, E.; Meyer, T. J. *J. Phys. Chem.* **1988**, *92*, 3708.
(44) Chen, P.; Curry, M.; Meyer, T. J. *Inorg. Chem.* **1989**, *28*, 2271.
(45) For the sake of simplicity one can take into account a reduced C_{2v} symmetry for the Ru–trpy type fragment, with the ligand lying on the *yz* plane and the *z* axis bisecting it. In this case, only between the d_{xz} metal orbital and the central N orbital contribution to the ligand LUMO, there is a substantial non-zero orbital overlap, as required for a d → LUMO CT transition.[35,44] Both of the involved orbitals belong to the b_1 representation, and optical CT is only allowed along the $z(a_1)$ direction as $b_1 \times b_1 = a_1$.

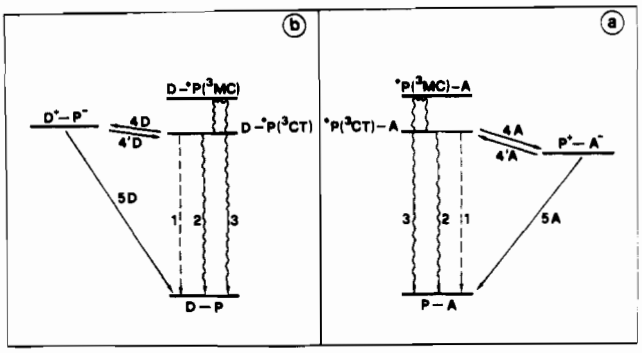

Figure 6. Schematic energy-level diagram for the P–A (a) and D–P (b) dyads.

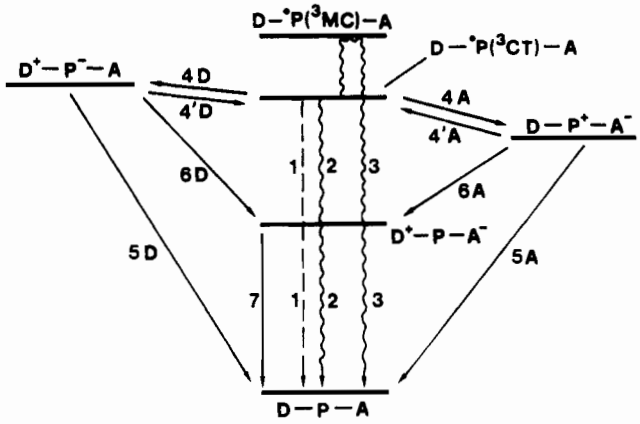

Figure 7. Schematic energy-level diagram for the D–P–A triads.

related MLCT transitions are therefore expected, while the intensity of the absorption band should be greater for the latter case. Comparison of the spectroscopic properties for $Ru(trpy)_2^{2+}$ and $Ru(ttp)_2^{2+}$ (Table II) indicates a small red shift and a substantially larger molar absorption coefficient for the latter compound, thus confirming that light absorption actually leads to electron promotion to a ligand system that includes the tolyl fragment.[32] This supports the component subdivision of the reported supramolecular systems, which is based on $Ru(ttp)_2^{2+}$ as a photosensitizer. Similar conclusions were reached by studying the influence on the intensity of the absorption bands of geometrical restraints and of electron-withdrawing and electron-repelling groups attached to remote positions of ttp.[46]

As happens for the other Ru(II)–polypyridine complexes,[11] light excitation in the spin-allowed metal-to-ligand CT bands eventually leads to the population of the lowest energy, usually luminescent ^{3}CT level. The lack of room-temperature luminescence for the isolated photosensitizer is explained by the presence of metal-centered (^{3}MC, of d → d orbital origin) excited states close in energy to the luminescent ^{3}CT excited state.[31,32,47] The ^{3}MC states, in fact, are strongly distorted with respect to the ground state and, once thermally populated from the ^{3}CT level, can undergo fast deactivation via nonradiative paths (including ligand release).[11,48] The energy level of the ^{3}MC states depends on the strength of the ligand field, which is related to the molecular structure of the ligand. Molecular models show that, contrary to what happens for bidentate ligands like 2,2′-bipyridine, tridentate trpy-type ligands are unable to coordinate in accord with the regular octahedral geometry, which is needed to have a strong ligand field in Ru(II) complexes. Thus, the energy gap between ^{3}MC and ^{3}CT in $Ru(ttp)_2^{2+}$ is small (~1800 cm^{-1} in nitrile solution[49]), and in fluid solution at high temperatures the ^{3}MC level can be easily populated. This offers a path to fast radiationless decay of the luminescent level. However, when the temperature is low and/or the environment is rigid, this path becomes less important because of the low thermal energy available and the constraints imposed to the nuclear motions. Under such conditions, luminescence can be observed.

As one can see from the absorption and luminescence (at 90 K) results shown in Tables II and III, the attachment of MV^{2+} and PTZ groups does not substantially influence the spectroscopic properties of the $Ru(ttp)_2^{2+}$ unit. This can be explained in terms of the presence of the $-CH_2-$ spacer between the two components. On the contrary, DPAA is directly linked to $Ru(ttp)_2^{2+}$, and therefore the interaction is larger. This leads to sizable changes of the spectroscopic properties. The same conclusions can be drawn from the comparison of the luminescence lifetimes in frozen solution at 90 K (Table III).

Mechanism of the Photoinduced Processes. Schematic energy-level diagrams for the P–A dyad, the D–P dyads, and the D–P–A triads are shown in Figures 6 and 7. Approximate values for the energy of *P(^{3}CT) in the various supramolecular species (1.89 eV for the species containing DPAA, 1.96 eV for the other species) can be obtained from the maxima of the luminescence bands at 90 K. The energies of the charge-separated states can be evaluated from the potentials shown in Table I: $Ru(ttp)_2^{3+}$–MV^+, 1.63 eV; PTZ^+–$Ru(ttp)_2^+$, 2.06 eV; $DPAA^+$–$Ru(ttp)_2^+$, 2.04 eV; PTZ^+–$Ru(ttp)_2^{2+}$–MV^+, 1.15 eV; $DPAA^+$–$Ru(ttp)_2^{2+}$–MV^+, 1.15 eV. It should be pointed out that the potential values have been measured in acetonitrile at room temperature, whereas the photoinduced processes have been studied in a propionitrile–butyronitrile mixture at 150 and 200 K. For this reason, as well as for the different stabilization and Coulombic terms for the one-electron-oxidized or -reduced species and the charge-separated species, the above values have to be considered as estimates and cannot be used too strictly in the discussion of the results.[5] The energy ordering shown in Figures 6 and 7 is qualitatively that expected from the spectroscopic and electrochemical data. The ^{3}MC level of the photosensitizer, which plays an important role in the deactivation of the luminescent level (vide supra), is also shown in those figures. The upper ^{1}LC and ^{1}CT energy levels of the photosensitizer, which are those directly obtained upon light excitation, are not shown since they are expected to undergo fast radiationless decay to the lowest excited state.[11,48]

In a rigid matrix at 90 K, no electron-transfer quenching is observed in all cases. This can be explained by the block of solvent repolarization and the consequent lack of stabilization of the electron-transfer "products", which makes the electron-transfer quenching thermodynamically forbidden in all our cases.[43] The following discussion will concern the behavior of the various systems at 150 and 200 K, where the luminescence of the isolated photosensitizer can be observed and the solvent is fluid.

$Ru(ttp)_2^{2+}$–MV^{2+} Dyad. The transient absorption spectrum at 150 K, Figure 4, shows that the reduced acceptor A^- (i.e., MV^+) is formed within 30 ns after the end of the laser pulse. As mentioned above, spectral overlapping does not allow one to establish the yield of charge separation. Once formed, the charge-separated (CS) state decays with τ = 4 μs, which is comparable with the lifetime of luminescence decay (Table III). It should be noted that the presence of MV^{2+} has little (if any) effect on the luminescence intensity of the photosensitizer and that at 150 K, and even more at 200 K, the luminescence lifetime of the dyad is *longer* than that of the isolated photosensitizer. These results suggest that the charge recombination reaction 5A, which leads to the ground state, is slower than the charge recombination reaction 4′A, which leads back to the excited state (Figure 6a). Therefore, the CS state is in equilibrium with the ^{3}CT level and decays mainly via the ^{3}MC one. The reason why reaction 5A is slow is 2-fold: (i) it falls in the Marcus inverted region (high exoergonicity and small intrinsic barrier[50]); (ii) its

(46) Thummel, R. P.; Hedge, V.; Jahng, Y. *Inorg. Chem.* **1989**, *28*, 3264.
(47) Kirchhoff, J. R.; McMillin, D. R.; Marnot, P. A.; Sauvage, J. P. *J. Am. Chem. Soc.* **1985**, *107*, 1138.
(48) Meyer, T. J. *Pure Appl. Chem.* **1986**, *58*, 1193.
(49) Unpublished results from our laboratories.

(50) ΔG° = −1.6 eV; for an analogous CS reaction the reorganization energy has been evaluated to be ~0.85 eV.[38] See also refs 51 and 52.

electronic factor is small because the reaction implies the transfer of an electron from A^- (i.e., MV^+) to the metal ion of P. Reaction 4'A, which is apparently faster, has a much larger electronic factor since the electron has to be transferred from A^- to the nearby ttp ligand of P. In order to occur in the microsecond time scale at 150 K, however, reaction 4'A must be considerably less endoergonic than it would appear ($\Delta G^\circ = +0.33$ eV) from the crude electrochemical data. In conclusion, in this dyad the CS state plays the role of a temporary parking place of the excited species. Being at lower energy than ^{3}CT, such a CS state reduces the Boltzmann population of the upper ^{3}MC level and therefore "protects" the ^{3}CT luminescent level from the fast, thermally activated radiationless decay via ^{3}MC.

PTZ–Ru(ttp)$_2^{2+}$ Dyad. For this dyad neither luminescence quenching nor changes in transient absorption compared to the isolated Ru(ttp)$_2^{2+}$ photosensitizer were observed. This implies that either reaction 4D in Figure 6b is slow compared with the intrinsic decay of the ^{3}CT level of the photosensitizer or the equilibrium between the CS state and ^{3}CT is strongly displaced toward the ^{3}CT level. In view of the results obtained for the DPAA–Ru(ttp)$_2^{2+}$ dyad (vide infra), the former explanation seems more plausible. Reaction 4D, in fact, is expected to be slow not only because it may be slightly endoergonic but mainly because it implies the transfer of an electron from PTZ, separated from the ttp ligand by a $-CH_2-$ group, to the metal ion of the photosensitizer.

DPPA–Ru(ttp)$^{2+}$ Dyad. For this system the results obtained can be summarized as follows: (i) sizable perturbations of the absorption and luminescence spectra of the photosensitizer; (ii) strong quenching of the luminescence intensity of the photosensitizer at 150 K; (iii) formation of a transient spectrum (related to charge separation, see below) within the laser pulse (20 ns); (iv) decay of the transient spectrum with $\tau = 450$ ns at 150 K; (v) biexponential decay of the luminescence. As expected on the basis of the molecular structure and shown by the results under point i, the photosensitizer and the electron donor are strongly coupled, contrary to what happens in the dyads described above. It follows that also the transient spectrum assigned to the CS state does not correspond to the sum of the spectra of the $DPAA^+$ and P^- components. Such an intercomponent coupling apparently makes reaction 4D (Figure 6b), which involves the transfer of an electron from DPAA to the oxidized metal, fast enough to produce a noticeable fraction of CS species within the excitation pulse. The other important point is that reaction 5D is fast enough to substantially contribute to the excited-state decay. Reaction 5D may be relatively fast for the following reasons: (a) the electronic factor is very favorable because of the strong D–P interaction; (b) the reorganizational energy associated with amine oxidation[51,52] can partly compensate for the large exoergonicity, placing the process in a not too "inverted" kinetic regime. As far as the presence of a minor, long-lived component is concerned, it could be related to the presence of a small fraction of conformers, with geometry unfavorable to electron transfer.

PTZ–Ru(ttp)$_2^{2+}$–MV^{2+} Triad. As shown by Figure 7, the energy-level diagram for the triads is not simply the superposition of the energy-level diagrams of the two parent dyads (Figure 6). The lowest excited level of the triads, in fact, is the fully CS level D^+–P–A^-, whose energy is about 1.1 eV above the ground state. The presence of this level offers two new pathways, 6A and 6D, for the decay of the partially CS states D–P^+–A^- and D^+–P^-–A. The fully charge-separated level can then be directly converted to the ground state via the charge-recombination reaction 7. In spite of the presence of such new deactivation pathways, the PTZ–Ru(ttp)$_2^{2+}$–MV^{2+} triad behaves like the Ru(ttp)$_2^{2+}$–MV^{2+} dyad. The lack of any effect by reaction 6D is easily accounted for because the D^+–P^-–A level cannot be populated, as shown by the results obtained for the PTZ–Ru(ttp)$_2^{2+}$ dyad (vide supra). The ineffectiveness of reaction 6A must be related to its very unfavorable electronic factor. Reaction 6A, in fact, involves the transfer of an electron from PTZ, which is connected to a ttp ligand via a $-CH_2-$ bridge, to the metal ion of the photosensitizer, exactly as reaction 4D, which is also ineffective (see the PTZ–Ru(ttp)$_2^{2+}$ dyad).

DPAA–Ru(ttp)$_2^{2+}$–MV^{2+} Triad. As shown in Figure 4, the transient spectrum of this triad is quite similar to that of the DPAA–P dyad. It should be noted however that formation of small amounts (10–20%) of MV^+ might have escaped observation because of spectral overlaps. The faster decay of the luminescence and transient absorption ($\tau = 100$ ns) for this triad compared to the parent DPAA–Ru(ttp)$_2^{2+}$ dyad must be related to the presence of the D^+–P–A^- level. In fact, reaction 6A is now expected to be very fast (in particular, much faster than reaction 5A) because of the good electronic factor (since the electron transfer to the metal ion of the photosensitizer involves the strongly coupled DPAA moiety) and the not too high exoergonicity ($\Delta G^\circ \sim -0.5$ eV). Reaction 6D ($\Delta G^\circ \sim 0.85$ eV) must also be faster than reaction 5D ($\Delta G^\circ \sim 2.0$ eV) because of the lower exoergonicity. As mentioned above, the initial transient spectrum is consistent with excited-state decay mainly through formation of D^+–P^-–A. Its decay, however, does not lead to D^+–P–A^-, since no recovery of the bleaching is detected before the decay of the D^+ and A^- absorption, but is consistent with the direct recovery of the D–P–A ground state. This suggests that the fully charge-separated state, D^+–P–A^-, does not accumulate, implying that reaction 7 is faster than reactions 6A and 6D. The involvement of the fully charge-separated state in the decay process, however, can be inferred from the increase in the decay rate. Direct electronic coupling between D^+ and A^- should be rather small, but coupling via superexchange interaction[53,54] involving D–P^+–A^- and D^+–P^-–A, which are very close in energy, can be large. Anyway, since reactions 6A and 6D are not expected to have electronic factors worse than that of reaction 7, the faster rate of the latter must be related to a better nuclear factor. A comparison with "analogous" systems (having different geometry and flexibility[13,42]) shows that the primary electron-transfer processes are much slower in our case. In the bpy-based systems[13,42] the observation of short-lived (30–150 ns) CS transients is allowed by the very fast rate of population of this state.

Conclusions. Five supramolecular systems (three dyads and two triads), consisting of a photosensitizer (P) linked to an electron acceptor (A) and/or an electron donor (D), have been synthesized by assembling derivatized terpyridine moieties around the Ru^{2+} ion (Figure 1). Fine chromatographic separations allow preparation of high purity samples of the various species (yields of 5–37%). The bis(terpyridine)ruthenium(II) core provides a pseudoaxial symmetry and great rigidity to the dyad and triad species. In the triads, the electron-acceptor (MV^{2+}) and -donor ($-CH_2$–PTZ or –DPAA) groups are 21 Å apart (edge-to-edge). In the PTZ–Ru(ttp)$_2^{2+}$ dyad, neither quenching of the photosensitizer luminescence nor formation of oxidized donor is observed. In the DPAA–Ru(ttp)$_2^{2+}$ dyad, luminescence quenching and transient formation of the oxidized donor take place. For the Ru(ttp)$_2^{2+}$–MV^{2+} dyad, transient formation of the reduced acceptor is observed, but the lifetime of the photosensitizer luminescence *increases*, indicating that charge recombination leads back to the excited photosensitizer. For the D–Ru(ttp)$^{2+}$–MV^{2+} triads (D = $-CH_2$–PTZ or –DPAA), a completely different behavior is observed. When D = $-CH_2$–PTZ, no pathway for the decay of *P via photoinduced CS is operative, while for D = –DPAA deactivation of *P via CS is at least 20 times faster than the intramolecular deactivation of *P. Since the two different donors have the same oxidation potential and CS involves similar reorganization energies (mostly of solvent origin[51,52]), the different behavior can be attributed to more favorable electronic factors for CS in the case of –DPAA. For the triad containing the –DPAA donor, however, CR is also fast and formation and decay

(51) Chen, J.-M.; Ho, T.-I.; Mou, C.-Y. *J. Phys. Chem.* **1990**, *94*, 2889.
(52) Finckh, P.; Heitele, H.; Volk, M.; Michel-Beyerle, M. E. *J. Phys. Chem.* **1988**, *92*, 6584.
(53) Wasielewsky, M. R.; Niemczyk, M. P.; Johnson, D. G.; Svec, W. A.; Minsek, D. W. *Tetrahedron* **1989**, *45*, 4785.
(54) McConnel, H. H. *J. Chem. Phys.* **1961**, *35*, 508.

of the fully charge separated D^+-P-A^- species cannot be time-resolved.

Better results (i.e., a higher efficiency of formation and a longer lifetime for D^+-P-A^-) could perhaps be obtained by modifying the DPAA-$Ru(ttp)_2^{2+}$-MV^{2+} system as follows: (i) to use a slightly better donor than -DPAA, in order to increase the rate of reaction 4'D; (ii) to use an acceptor more difficult to reduce than $-MV^{2+}$, so as to increase the energy gap between D^+-P-A^- and the ground state, which would decrease the rate of the CR reaction 7 (Marcus inverted behavior); (iii) to increase the separation between P and MV^{2+}, so as to decrease the electronic factor for reaction 7.

Acknowledgment. We thank P. Staub, L. Minghetti, and G. Gubellini for technical assistance. This work was supported by the Centre Nationale de la Recherche Scientifique and Ministere de la Recherche (France) and by the Programma Finalizzato Chimica Fine II, Consiglio Nazionale delle Ricerche, and Ministero dell' Universitá e della Ricerca Scientifica e Tecnologica (Italy).

Registry No. ttp, 89972-77-0; ttp hydrobromide salt, 136247-29-5; $Fe(ttp)_2(PF_6)_2$, 136247-59-1; 6'-t-2,2':4',2''-tp, 136247-30-8; ttp-Br, 89972-78-1; ttp-MV^{2+}-$2NO_3^-$, 136247-31-9; ttp-MV^{2+}-$2Cl^-$, 136247-32-0; ttp-MV^{2+}-$2PF_6^-$, 136247-34-2; ttp-PTZ, 124598-56-7; ttp-DPAA, 136247-34-2; $Ru(ttp)Cl_3$, 136276-24-9; $[Ru(ttp)_2](PF_6)_2$, 121810-60-4; $[Ru(ttp)_2]^{3+}$, 121810-63-7; $[Ru(ttp)_2]^+$, 121810-62-6; $[PTZ\text{-}Ru(ttp)_2](PF_6)_2$, 136247-49-9; $[PTZ\text{-}Ru(ttp)_2]^{4+}$, 136247-42-2; $[PTZ\text{-}Ru(ttp)_2]^{3+}$, 136247-46-6; $[PTZ\text{-}Ru(ttp)_2]^+$, 136247-36-4; $[DPAA\text{-}Ru(ttp)_2](PF_6)_2$, 136247-51-3; $[DPAA\text{-}Ru(ttp)_2]^{4+}$, 136247-43-3; $DPAA\text{-}Ru(ttp)_2^{3+}$, 136247-45-5; $DPAA\text{-}Ru(ttp)_2^+$, 136276-21-6; $[Ru(ttp)_2\text{-}MV](PF_6)_4$, 136247-52-4; $[Ru(ttp)_2\text{-}MV]^{5+}$, 136247-58-0; $[Ru(ttp)_2\text{-}MV]^{3+}$, 136247-39-7; $[Ru(ttp)_2\text{-}MV]^+$, 136247-35-3; $Ru(ttp\text{-}MV^{2+})_2(PF_6)_6$, 136247-54-6; $[PTZ\text{-}Ru(ttp)_2\text{-}MV](PF_6)_4$, 136247-55-7; $[PTZ\text{-}Ru(ttp)_2\text{-}MV]^{6+}$, 136276-22-7; $[PTZ\text{-}Ru(ttp)_2\text{-}MV]^{5+}$, 136247-47-7; $[PTZ\text{-}Ru(ttp)_2\text{-}MV]^{3+}$, 136247-40-0; $[PTZ\text{-}Ru(ttp)_2\text{-}MV]^+$, 136247-37-5; $[DPAA\text{-}Ru(ttp)_2\text{-}MV](PF_6)_4$, 136247-57-9; $[DPAA\text{-}Ru(ttp)_2\text{-}MV]^{6+}$, 136247-44-4; $[DPAA\text{-}Ru(ttp)_2\text{-}MV]^{5+}$, 136276-23-8; $[DPAA\text{-}Ru(ttp)_2\text{-}MV]^{3+}$, 136247-41-1; $[DPAA\text{-}Ru(ttp)_2\text{-}MV]^+$, 136247-38-6; acetamide, 60-35-5; *p*-tolylaldehyde, 104-87-0; 2-acetylpyridine, 1122-62-9; Mohr's salt, 10045-89-3; 1-methyl-4,4'-bipyridinium iodide, 38873-01-7; phenothiazine, 92-84-2; 4-(*N*,*N*-di-*p*-anisoylamino)benzaldehyde, 89115-20-8.

Contribution from the Departments of Chemistry, McMaster University, Hamilton, Ontario L8S 4M1, Canada, and University of Toronto, Toronto, Ontario M5S 1A1, Canada

Crystal Structures of Potassium Cryptated Salts of the $TeSe_2^{2-}$, Pyramidal $TeSe_3^{2-}$, and Mixed Compounds Containing Pyramidal $TeSe_3^{2-}$ and Chain $Te_xSe_{4-x}^{2-}$ Anions and ^{77}Se and ^{125}Te Solution NMR Studies of the Pyramidal Selenothiotellurite Anions $TeS_mSe_{3-m}^{2-}$ (m = 0-3)

Mår Björgvinsson,[1a] Jeffery F. Sawyer,*[1b] and Gary J. Schrobilgen*[1a]

Received August 9, 1990

The preparation of several compounds containing mixed tellurium-selenium and tellurium-sulfur-selenium anions as cryptated potassium salts [crypt ≡ 4,7,13,16,21,24-hexaoxa-1,10-diazabicyclo[8.8.8]hexacosane] are reported along with the X-ray crystal structures of four compounds (**1**-**4**) containing Te-Se dianions. Compound **1** (2,2,2-crypt-$K^+)_2TeSe_2^{2-}$-en, crystallizes in the triclinic space group $P\bar{1}$ with a = 10.9725 (8) Å, b = 12.1940 (9) Å, c = 12.3242 (10) Å, α = 59.182 (7)°, β = 73.781 (7)°, γ = 67.718 (6)°, V = 1303 Å^3, D_x = 1.500 g cm^{-3} for Z = 1, and R (R_w) = 0.0382 (0.0465) for 4459 observed [$I \geq 3\sigma(I)$] data. Similarly, compound **2**, (2,2,2-crypt-$K^+)_2TeSe_3^{2-}$-en, crystallizes in the trigonal space group $P3_2$ (No. 145) with a = 12.386 (5) Å, c = 30.669 (15) Å, V = 4076 Å^3, D_x = 1.537 g cm^{-3} for Z = 3, and R (R_w) = 0.0574 (0.0638) for 1810 observed [$I \geq 2.5\sigma(I)$] data. However, compounds **3** and **4** were found to be mixed crystals containing principally the pyramidal $TeSe_3^{2-}$ anion as well as different minor amounts of a chain tetrachalcogen anion, although the overall Te/Se composition of the averaged anion in each compound is essentially constant for the two compounds at $Te_{0.9}Se_{3.4}^{2-}$. Compound **3** [values for **4** in brackets] crystallizes in the monoclinic space group $P2_1/n$ (No. 14) with a = 12.252 (4) Å [12.286 (2) Å], b = 21.643 (3) Å [21.587 (9) Å], c = 20.718 (3) Å [20.759 (2) Å], β = 97.45 (2)° [97.61 (1)°], V = 5447 Å^3 [5457 Å^3], and R (R_w) = 0.0733 (0.0730) [0.0667 (0.0632)] for 2150 [2898] observed reflections. In **1**, the Te-Se bond lengths and Se-Te-Se bond angle in the $TeSe_2^{2-}$ anion are 2.501 (1) and 2.504 (1) Å and 111.3 (1)°, respectively, while in **2** the Te-Se bond lengths in the pyramidal $TeSe_3^{2-}$ anion are 2.454 (4), 2.460 (4), and 2.465 (4) Å and the Se-Te-Se bond angles are 104.8 (2), 107.4 (1), and 108.9 (1)°. In compound **3**, the anion site consists of ca. 89% of a pyramidal anion (assumed to be $TeSe_3^{2-}$) and 11% of an open-chain tetrachalcogen anion with all compositions *except* $TeSe_3^{2-}$ being predicted on the basis of NMR data (see preceding paper), while in **4** the pyramidal:chain dianion ratio is ca. 81:19. In addition, the pyramidal-shaped selenothiotellurite anions $TeS_mSe_{3-m}^{2-}$ (m = 0-3) have been prepared and characterized in ethylenediamine (en) solutions. Trends in the ^{77}Se and ^{125}Te chemical shifts and in the one-bond spin-spin coupling constants, $^1J(^{125}Te - ^{77}Se)$, for the latter species are reported and discussed in terms of the relative electronegativities of sulfur and selenium.

Introduction

In recent years, a large number of homopolychalcogenide anions of selenium and tellurium have been structurally characterized in the solid state.[2-10] However, the heteropolychalcogenide anions of Se and Te have been much less studied. Greiver et al.[11] have reported on the preparation and isolation of the salts of $TeSe_2^{2-}$ and $TeSe_3^{2-}$. However, only the mixed Se/Te polychalcogenide Rb_2TeSe_4 had been structurally characterized in the solid state at the start of this study.[12] More recently, however, structures of Na_2TeSe_3 and K_2TeSe_3 have been reported[13a] along with preliminary details for the compounds $[Sr(en)_4]TeSe_3$ and $[Ba(en)_{3,5}]TeSe_3$ (en = ethylenediamine),[13b] all of which contain the pyramidal $TeSe_3^{2-}$ anion. The latter abstract also includes some information on the salts (2,2,2-crypt-K)$_2TeSe_{10}$ and [(2,2,2-crypt-Ba)(en)]$TeSe_{10}$·0.5en (2,2,2-crypt = 4,7,13,16,21,24-hex-

(1) (a) McMaster University. (b) University of Toronto.
(2) Zagler, R.; Eisenmann, B.; Schäfer, H. *Z. Naturforsch.* **1987**, *42B*, 151.
(3) Teller, R. G.; Krause, L. J.; Haushalter, R. C. *Inorg. Chem.* **1983**, *22*, 1809.
(4) Böttcher, P. *Z. Anorg. Allg. Chem.* **1977**, *432*, 167.
(5) Devereux, L. A.; Sawyer, J. F.; Schrobilgen, G. J. *Acta Crystallogr.* **1985**, *C41*, 1730.
(6) König, T.; Eisenmann, B.; Schäfer, H. *Z. Anorg. Allg. Chem.* **1983**, *498*, 99.
(7) Brese, N. E.; Randall, C. R.; Ibers, J. A. *Inorg. Chem.* **1988**, *27*, 940.
(8) König, T.; Eisenmann, B.; Schäfer, H. *Z. Naturforsch.* **1982**, *37B*, 1245.
(9) Cisar, A.; Corbett, J. D. *Inorg. Chem.* **1977**, *16*, 632.
(10) Huffman, J. C.; Haushalter, R. C. *Z. Anorg. Allg. Chem.* **1984**, *518*, 203.
(11) Greiver, T. N.; Sal'dau, É. P.; Zaitseva, I. G. *J. Appl. Chem. USSR (Engl. Transl.)* **1971**, *44*, 1502.
(12) Böttcher, P.; Kretschmann, U. *Z. Naturforsch.* **1985**, *40b*, 895.
(13) (a) Zagler, R.; Eisenmann, B. *Z. Kristallogr.* **1988**, *183*, (b) *Ibid.* **1988**, *185*, 473.

0020-1669/91/1330-4238$02.50/0